Diabetologia (2009) 52:347–358
DOI 10.1007/s00125-008-1215-5

ARTICLE

Role of MKK3–p38 MAPK signalling in the development of type 2 diabetes and renal injury in obese *db/db* mice

A. K. H. Lim · D. J. Nikolic-Paterson · F. Y. Ma · E. Ozols · M. C. Thomas · R. A. Flavell · R. J. Davis · G. H. Tesch

Received: 19 August 2008 / Accepted: 27 October 2008 / Published online: 9 December 2008

Abstract
Aims/hypothesis Obesity and diabetes are associated with increased intracellular p38 mitogen-activated protein kinase (MAPK) signalling, which may promote tissue inflammation and injury. Activation of p38 MAPK can be induced by either of the immediate upstream kinases, MAP kinase kinase (MKK)3 or MKK6, and recent evidence suggests that MKK3 has non-redundant roles in the pathology attributed to p38 MAPK activation. Therefore, this study examined whether MKK3 signalling influences the development of obesity, type 2 diabetes and diabetic nephropathy.
Methods Wild-type and *Mkk3* (also known as *Map2k3*) gene-deficient *db/db* mice were assessed for the development of obesity, type 2 diabetes and renal injury from 8 to 32 weeks of age.
Results $Mkk3^{+/+}$ *db/db* and $Mkk3^{-/-}$ *db/db* mice developed comparable obesity and were similar in terms of incidence and severity of type 2 diabetes. At 32 weeks, diabetic $Mkk3^{+/+}$ *db/db* mice had increased kidney levels of phospho-p38 and MKK3 protein. In comparison, kidney levels of phospho-p38 in diabetic $Mkk3^{-/-}$ *db/db* mice remained normal, despite a fourfold compensatory increase in MKK6 protein levels. The reduced levels of p38 MAPK signalling in the diabetic kidneys of $Mkk3^{-/-}$ *db/db* mice was associated with protection against the following: declining renal function, increasing albuminuria, renal hypertrophy, podocyte loss, mesangial cell activation and glomerular fibrosis. Diabetic $Mkk3^{-/-}$ *db/db* mice were also significantly protected from tubular injury and interstitial fibrosis, which was associated with reduced *Ccl2* mRNA expression and interstitial macrophage accumulation.
Conclusions/interpretation MKK3–p38 MAPK signalling is not required for the development of obesity or type 2 diabetes, but plays a distinct pathogenic role in the progression of diabetic nephropathy in *db/db* mice.

Keywords *db/db* mice · Diabetes · Diabetic nephropathy · Macrophage · MCP-1 · MKK3 · p38 MAPK · Podocyte

Abbreviations

gcs	glomerular cross-sections
MAPK	mitogen-activated protein kinase
MCP-1	monocyte chemoattractant protein-1
MKK	MAP kinase kinase
PLP	paraformaldehyde–lysine–periodate
tcs	tubular cross-sections
WT	Wilm's tumour

A. K. H. Lim · D. J. Nikolic-Paterson · F. Y. Ma · E. Ozols · G. H. Tesch (✉)
Department of Nephrology, Monash Medical Centre,
246 Clayton Road,
Clayton, VIC 3168, Australia
e-mail: greg.tesch@med.monash.edu.au

A. K. H. Lim · D. J. Nikolic-Paterson · G. H. Tesch
Department of Medicine, Monash University,
Clayton, VIC, Australia

M. C. Thomas
Baker Research Institute,
Melbourne, VIC, Australia

R. A. Flavell
Yale University School of Medicine,
New Haven, CT, USA

R. J. Davis
Howard Hughes Medical Institute,
University of Massachusetts Medical School,
Worcester, MA, USA

Introduction

Inflammation and cellular dysfunction are features of obesity, diabetes and diabetic nephropathy, which are associated with intracellular activation of mitogen-activated protein kinase (MAPK) signalling pathways. Components of the diabetic milieu, including hyperglycaemia, hyperlipidaemia, hyperinsulinaemia, reactive oxygen species, AGE, angiotensin II and proinflammatory cytokines, can stimulate increased MAPK signalling in cells and may thereby promote tissue injury [1].

p38 MAPK signalling is known to promote inflammatory and profibrotic responses and has been associated with other cellular functions such as glucose uptake, cell differentiation, apoptosis and proliferation [2–4]. Levels of activated p38 are elevated in the skeletal muscle, adipose tissue and kidneys of diabetic patients [5–7], suggesting that some p38 responses may be important for the pathogenesis of diabetes and its complications. Functional blocking studies in animal models have demonstrated that p38 signalling induces the inflammation in insulitis and diabetic cardiomyopathy [8, 9]. Furthermore, in vitro experiments have shown that p38 inhibition can suppress adipogenesis, prevent insulin resistance in myotubes exposed to TNF-α or oxidative stress and stimulate glucose transport in adipocytes [10, 11]; however, these findings remain controversial.

Clinical studies have demonstrated that kidney p38 activity is increased and associated with the development of diabetic nephropathy [5, 12]. Renal biopsies from patients with established type 2 diabetes display prominent p38 signalling despite treatment with angiotensin system inhibitors [5]. In comparison, animal models of diabetes have shown that p38 activation rapidly increases in glomeruli and tubules in response to hyperglycaemia and occurs in the accumulating kidney interstitial cells associated with advanced nephropathy. Pharmacological blockade of p38 is known to suppress the development of inflammation and fibrosis in acute kidney disease [13, 14]. These mechanisms are also important in the progression of diabetic renal injury, suggesting that diabetic nephropathy may also be suppressed by inhibiting p38 signalling.

In vitro studies have identified specific kidney cells and mechanisms of renal injury that may be affected by p38 signalling during diabetes. Exposure to high glucose activates p38 in human mesangial cells [15], mouse podocytes [16] and rat proximal tubular cells [17]. Similarly, glycated albumin can stimulate p38 phosphorylation in cultured fibroblasts [18]. Activation of p38 induces apoptosis of rat mesangial cells exposed to methylglyoxal [19] and apoptosis of mouse podocytes following stimulation with TGF-β [20] and AGE [21, 22]. In addition, p38 signalling can contribute to proinflammatory and profibrotic responses. Activation of p38 enhances production of monocyte chemoattractant protein-1 (MCP-1) by vascular endothelial cells [23], induces local angiotensinogen production in rat tubular cells [17], stimulates both TGF-β-induced fibronectin accumulation in renal interstitial fibroblasts [24] and collagen production in mouse mesangial cells [25], increases *Tgf-β1* (also known as *Tgfb1*) expression in renal tubular cells [26] and promotes synthesis of vascular endothelial growth factor induced by angiotensin II [27, 28]. Studies have also shown that p38 signalling mediates both tubular hypertrophy induced by high glucose [26] and transactivation of the epidermal growth factor receptor required for dedifferentiation of proximal tubular epithelial cells following oxidant injury [29].

Functional blocking studies are required to determine the role of p38 signalling in diabetes and its complications. One strategy for achieving this goal is to perform studies of diabetes in a mouse strain that is genetically deficient in one of the immediate upstream kinases (MAP kinase kinase [MKK]3 or MKK6) that regulate p38 signalling. These protein kinases provide a parallel and independent mechanism of phosphorylating p38 but their relative contribution to the increased p38 activity associated with diabetic nephropathy is unknown. Genetically modified *Mkk3*$^{-/-}$ and *Mkk6*$^{-/-}$ mice are viable and fertile, and provide an opportunity to study the role of p38 signalling in models of disease. Of these two kinases, MKK3 appears to be the most attractive target for studies of genetic deletion, because MKK3–p38 signalling has been shown to be non-redundant in some pathological processes [30, 31]. Furthermore, mouse studies have shown that *Mkk3* deficiency is protective in models of passive arthritis and streptozotocin-induced pancreatic inflammation [32, 33].

In the current study, *Mkk3*-deficient *db/db* mice were created and used to examine the role of MKK3–p38 signalling in the development of obesity, hyperglycaemia and nephropathy in the *db/db* model of type 2 diabetes.

Methods

Animal model Obese (*db/db*) and lean *db/+* heterozygote control mice were created by breeding pairs of C57BL/6 *db/+* mice obtained from Jackson Laboratories (Bar Harbor, ME, USA) and were genotyped for the mutated leptin receptor. *Mkk3*$^{-/-}$ mice [34] were back-crossed for eight generations on to the C57BL/6 strain and bred at Monash Medical Centre (Clayton, VIC, Australia). *Mkk3*$^{-/-}$ mice were then crossed with C57BL/6 *db/+* mice to create *Mkk3*$^{-/-}$ *db/+* mice, which were validated by genotyping. The latter were then interbred to create *Mkk3*$^{-/-}$ *db/db* mice. Only males were used for the study due to the higher

incidence of diabetes. Mice were maintained on a normal diet under standard animal housing conditions.

The development of obesity and diabetes was examined in groups of *Mkk3*$^{+/+}$ and *Mkk3*$^{-/-}$ *db/db* mice (n=33–40) between 8 and 32 weeks of age, with monthly assessment of weight and blood glucose (Medisense glucometer; Abbott Laboratories, Bedford, MA, USA). Insulin and glucose tolerance tests (described below) were performed at 8 and 32 weeks. Subgroups of the *Mkk3*$^{+/+}$ and *Mkk3*$^{-/-}$ *db/db* mice (n=10), which showed equivalent levels of diabetes from 12 to 32 weeks, were used to examine the development of diabetic nephropathy and kidney p38 signalling. The urine albumin excretion rate was measured at 8, 16, 24 and 32 weeks. Renal function was determined at 32 weeks. Groups of age-matched non-diabetic *Mkk3*$^{+/+}$ and *Mkk3*$^{-/-}$ *db/+* mice (n=8–10) were also studied as controls. Mice were killed at 32 weeks and selected organs (liver, kidneys and epididymal fat) were examined. Tissues were fixed in 4% (vol./vol.) neutral-buffered formalin or 2% (wt/vol.) paraformaldehyde–lysine–periodate (PLP) or were snap-frozen.

Approval for these studies was obtained from the Monash Medical Centre Animal Ethics Committee in accordance with the Australian Code of Practice for the Care and Use of Animals for Scientific Purposes, 7th edition (2004).

Glucose and insulin tolerance tests To test glucose tolerance, mice were given an intraperitoneal injection of D-glucose (1 g/kg) after a 12 h fast. For insulin tolerance, mice were injected with human insulin (2 U/kg; Actrapid, Novo Nordisk, Bagsvaerd, Denmark) after a 6 h fast. The tolerance profiles were assessed by measuring blood glucose at 0, 30, 60, 90 and 120 min, using the glucose oxidase method.

Biochemical analysis Urine was collected from mice housed in metabolism cages for 18 h. Whole blood was collected by cardiac puncture in anaesthetised mice, centrifuged (800 *g*, 10 min) and stored as serum or heparinised plasma. ELISA kits were used to measure urine albumin (Bethyl Laboratories, Montgomery, TX, USA) and plasma insulin (Linco Research, St Charles, MO, USA). Serum NEFA were assessed by a colorimetric assay kit (Wako Pure Chemical Industries, Osaka, Japan). HbA_{1c} was measured by HPLC in the Biochemistry Department at the Monash Medical Centre. Serum and urine creatinine were determined by HPLC and used to calculate creatinine clearance.

Histopathology analysis Formalin-fixed sections (2 μm) were stained with periodic acid–Schiff's reagent to assess structure and counterstained with haematoxylin to identify nuclei. Glomerular volume and matrix fraction were assessed by computer image analysis (Image-Pro Plus; Media Cybernetics, Silver Spring, MD, USA) and cellularity was assessed by counting nuclei in 20 hilar glomerular cross-sections (gcs) per animal. Tubular atrophy was assessed by counting injured (dilated, atrophied, necrotic) tubular cross-sections (tcs) in ten cortical fields (magnification: ×250) as a percentage of total tcs. Interstitial volume was assessed by point-counting in 20 fields (magnification: ×400). Staining for collagen was performed by immersing sections (4 μm) in 1% (wt/vol.) Picro-sirius red (Sirius Red; Sigma-Aldrich, St Louis, MO, USA) for 1 h and differentiating with 0.5% (vol./vol.) glacial acetic acid. Glomerular (20 hilar gcs) and interstitial staining (20 cortical fields, magnification: ×250, excluding blood vessels) were assessed by computer image analysis, as a percentage of area stained. All scoring was performed on blinded slides.

Antibodies The following primary antibodies were used in this study: rabbit anti-phospho (p)-p38 MAPK (Thr180/Tyr182), rabbit anti-phospho-MKK3/phospho-MKK6 (Ser189/207) and rabbit anti-cleaved caspase 3 (ASP175) (Cell Signaling, Beverly, MA, USA); mouse anti-p38α (Upstate Biotechnology, Lake Placid, NY, USA); rabbit anti-MKK3, goat anti-MKK6 and rabbit anti-Wilm's tumour (WT) antigen 1 (C-19) (Santa Cruz Biotechnology, Santa Cruz, CA, USA); rabbit anti-tubulin (Abcam, Cambridge, UK); mouse anti-α-smooth muscle actin (SMA) (1A4; Sigma-Aldrich); rat anti-mouse Ki67 (TEC-3; Dako, Carpinteria, CA, USA); and rat-anti CD68 (FA-11; Serotec, Oxford, UK).

Immunohistochemistry Immunostaining for phospho-p38, cleaved caspase-3, WT1 and Ki67 was performed on 4 μm formalin-fixed paraffin-embedded sections. Immunostaining for CD68 was performed on 5 μm PLP-fixed cryostat sections. For antigen retrieval (phospho-p38, cleaved caspase-3, WT1 and Ki67), dewaxed paraffin sections were heated in a microwave oven (800 W, 12 min) or pressure cooker (HIGH setting 20 min, full pressure 5 min) in 10 mmol/l sodium citrate buffer (pH 6.0). After cooling, sections were treated with 20% (vol./vol.) sheep serum or 20% (vol./vol.) rabbit serum for 30 min and then incubated overnight at 4°C with primary antibody in 3% (wt/vol.) BSA. Sections were then placed in 0.6% (vol./vol.) hydrogen peroxide in methanol for 20 min to inactivate endogenous peroxidase. For detection of α-SMA antibody, sections were incubated with peroxidase-conjugated sheep anti-mouse IgG (Dako), followed by mouse peroxidase-conjugated anti-peroxidase complexes (Dako). All other primary antibodies were detected using

a standard ABC-peroxidase system: avidin–biotin block, biotinylated antibodies (sheep anti-rabbit or rabbit anti-rat IgG) and ABC-peroxidase (Vector Laboratories, Burlingame, CA, USA). Sections were developed with 3,3-diaminobenzidine (Sigma) to produce a brown colour. CD68 sections were counterstained with haematoxylin to assist cell counting. Normal rabbit and goat serum or isotyped-matched irrelevant IgGs were used as negative controls.

Quantification of immunohistochemistry The number of phospho-p38-, WT1-, Ki67- and CD68-positive cells was counted in 20 hilar gcs per animal (magnification: ×400). The number of phospho-p38-positive tubules (>50% nuclei stained) was counted in 20 cortical fields (magnification: ×250) and expressed as a percentage of total tcs. Interstitial phospho-p38-positive and CD68-positive cells were counted in 50 cortical fields (magnification: ×400) and expressed as cells/mm^2. Cleaved caspase-3-positive tubular cells were counted in the entire kidney cortex and expressed as cells/mm^2. Cleaved caspase-3-positive glomerular cells were extremely rare and therefore not assessed. α-SMA staining was quantified by computer image analysis in 20 hilar gcs (magnification: ×400) and 20 cortical fields (magnification: ×250), and expressed as the percentage of area stained.

Western blotting Frozen kidney samples were homogenised in lysis buffer (pH 7.2) containing 8.1 mmol/l Na_2HPO_4, 1.5 mmol/l KH_2PO_4, 135 mmol/l NaCl, 2.7 mmol/l KCl, 1.0 mmol/l EDTA, 5 mmol/l NaF, 6 mol/l urea, 0.5% (vol./vol.) Triton-X-100, 1.0 mmol/l Na_3VO_4, 20 mmol/l sodium pyrophosphate, 25 μg/ml leupeptin, 3 μg/ml aprotinin, 100 μmol/l phenylmethylsulfonyl fluoride and 1% (vol./vol.) phosphatase inhibitor cocktail (Sigma-Aldrich). Samples were separated on a 4–20% (wt/vol.) SDS-PAGE gel and electro-transferred on to nitrocellulose membranes. Membranes were then blocked for 1 h with Odyssey blocking buffer (LICOR, Lincoln, NE, USA) and incubated overnight at 4°C with primary antibody in Odyssey buffer. Blots were then washed with Tris-buffered saline/0.1% (vol./vol.) Tween-20 and incubated for 1 h with secondary antibody (goat anti-rabbit or donkey anti-goat Alexa Fluor 680 [Invitrogen, Carlsbad, CA, USA]; or donkey anti-mouse IRDye 800 [Rockland, Gilbertsville, PA, USA]). After washing, protein bands were detected using the Odyssey Infrared Image Detection system (LICOR). α-Tubulin was used as a loading control. After detection of phospho-p38 and tubulin at 680 nm, blots were reprobed for p38α at 800 nm. Densitometry analysis was performed using Gel-pro Analyzer 3.0 software (Media Cybernetics). Results are expressed as the integrated optical density relative to tubulin.

Real-time RT-PCR Total RNA was extracted from whole-kidney samples using the RiboPure reagent (Ambion, Austin, TX, USA) and reverse-transcribed using a kit (Superscript First-Strand Synthesis kit; Invitrogen) with random primers. Real-time PCR was performed using the Rotor-Gene 3000 system (Corbett Research, Sydney, NSW, Australia) with thermal cycling conditions of 37°C for 10 min, 95°C for 5 min, followed by 50 cycles of 95°C for 15 s, 60°C for 20 s and 68°C for 20 s. The primer pairs and carboxyfluorescein-labelled minor groove binder probes used were: *Tnf-α* (also known as *Tnf*) (forward: GGC TGC CCC GAC TAC GT; reverse: TTT CTC CTG GTA

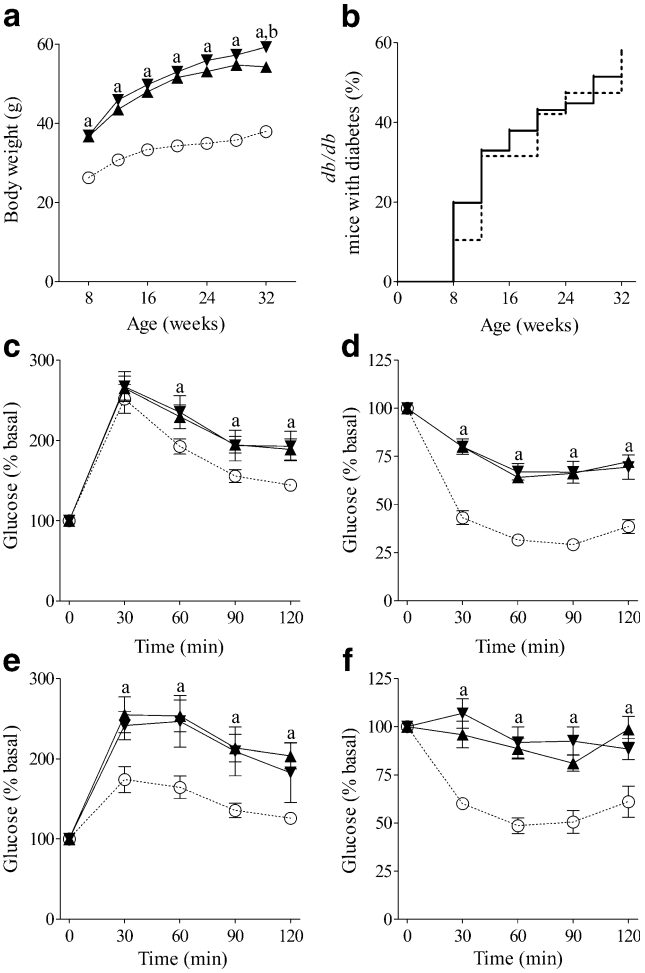

Fig. 1 Effect of MKK3 deficiency on obesity and type 2 diabetes. Serial measurements from 8 to 32 weeks of age show the development of **a** an equivalent obesity profile between *Mkk3*$^{+/+}$ *db/db* (upright triangles) and *Mkk3*$^{-/-}$ *db/db* mice (inverted triangles), which were 50% bigger than control *db/+* mice (circles) at 32 weeks, and **b** a similar incidence of diabetes between *Mkk3*$^{+/+}$ *db/db* (solid line) and *Mkk3*$^{-/-}$ *db/db* mice (dotted line) of 50% by 32 weeks. Glucose tolerance and insulin sensitivity tests performed at week 8 (**c**, **d**) and week 32 (**e**, **f**) show a similar progression of glucose intolerance and insulin resistance in *Mkk3*$^{+/+}$ *db/db* mice (upright triangles) and *Mkk3*$^{-/-}$ *db/db* (inverted triangles) compared with control *db/+* mice (circles). Data are means±SEM; n=33–40. [a]$p<0.001$ for *db/db* vs *db/+* mice; [b]$p<0.05$ for *Mkk3*$^{-/-}$ *db/db* vs *Mkk3*$^{+/+}$ *db/db* mice

Table 1 Physiological characteristics at 32 weeks

Characteristic	Mouse genotype			
	db/+		*db/db*	
	Mkk3$^{+/+}$	*Mkk3*$^{-/-}$	*Mkk3*$^{+/+}$	*Mkk3*$^{-/-}$
Body weight (g)	34.9±3.0	33.8±2.2	52.5±9.8[c]	59.9±5.4[c,d]
Liver/BW (%)	3.8±0.3	3.7±0.6	7.4±1.2[c]	6.2±1.3[c,d]
Epididymal fat/BW (%)	1.5±0.4	1.5±0.4	2.8±2.1[a]	2.7±0.6[a]
Serum NEFA (mmol/l)	0.64±0.31	0.63±0.11	1.17±0.21[b]	1.24±0.43[b]
Fasting insulin (pmol/l)	64±7	53±6	1920±140[c]	1890±40[c]

Data are mean±SEM, n=8–10 (*db/+* mice), n=33–40 (*db/db* mice)
[a] $p<0.05$, [b] $p<0.01$, [c] $p<0.001$ vs *Mkk3*$^{+/+}$ *db/+* mice
[d] $p<0.01$ vs *Mkk3*$^{+/+}$ *db/db* mice
BW, body weight

TGA GAT AGC AAA TC; probe: TCA CCC ACA CCG TCA G); *Ccl2* (forward: GAC CCG TAA ATC TGA AGC TAA; reverse: CAC ACT GGT CAC TCC TAC AGA A; probe: ACA ACC ACC TCA AGC AC); and *Tgf-ß1* (forward: GGA CAC ACA GTA CAG CAA; reverse: GAC CCA CGT AGT AGA CGA T; probe: ACA ACC AAC ACA ACC C). The relative amount of mRNA was calculated using comparative Ct (ΔΔCt) method. All specific amplicons were normalised against 18S rRNA, which was amplified in the same reaction as an internal control using commercial assay reagents (Applied Biosystems, Scoresby, VIC, Australia).

Statistical analysis Statistical differences were analysed by either the unpaired Student's *t* test or one way ANOVA with Tukey's multiple comparison post-test. Correlations were performed using Pearson's correlation coefficient. Data were recorded as mean±SEM with $p<0.05$ considered significant. All analyses were performed using GraphPad Prism 5.0 (GraphPad, San Diego, CA, USA).

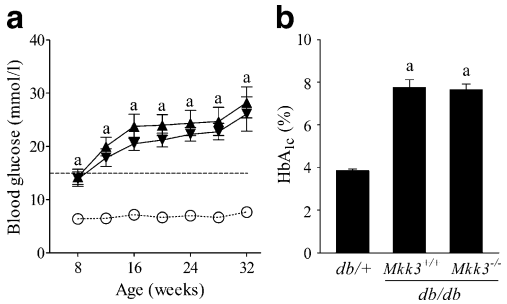

Fig. 2 Equivalent levels of hyperglycaemia in selected *db/db* mice. Diabetic *db/db* mice that were selected for analysis of kidney p38 activation and nephropathy had a similar fasting blood glucose profile, which showed a progressive increase of glycaemia from 8 to 32 weeks (**a**) and the equivalence between the two groups in hyperglycaemia was confirmed by HbA_{1c} measurement at 32 weeks (**b**). Triangles, *Mkk3*$^{+/+}$ *db/db*; inverted triangles, *Mkk3*$^{-/-}$ *db/db*; circles, control *db/+*. Data are means±SEM; n=10. [a] $p<0.001$ for *db/db* vs *db/+* mice. The dashed horizontal line represents the threshold level of blood glucose above which mice are considered diabetic

Results

Mkk3 deletion does not affect obesity or type 2 diabetes in db/db mice Between the age of 8 and 32 weeks, *Mkk3*$^{+/+}$ *db/db* and *Mkk3*$^{-/-}$ *db/db* mice developed comparable obesity and were 50% heavier than control *db/+* mice at 32 weeks (Fig. 1a). The incidence of diabetes (non-fasting blood glucose >16 mmol/l) was similar in *Mkk3*$^{+/+}$ *db/db* and *Mkk3*$^{-/-}$ *db/db* mice, reaching approximately 50% at 32 weeks (Fig. 1b). In addition, both *db/db* genotypes showed an equivalent impairment of glucose and insulin tolerance compared with *db/+* mice at 8 and 32 weeks (Fig. 1c–f). *Mkk3*$^{-/-}$ *db/db* mice showed less hepatomegaly than *Mkk3*$^{+/+}$ *db/db* mice at 32 weeks, but there was no significant difference in epididymal fat weight, plasma insulin or serum NEFA (Table 1).

Mkk3 deficiency reduces p38 MAPK activation in diabetic kidneys Diabetic *Mkk3*$^{+/+}$ and *Mkk3*$^{-/-}$ *db/db* mice selected for analysis of nephropathy had equivalent obesity (53.3±2.8 vs 58.5±1.9 g), fasting blood glucose profile and HbA_{1c} levels (Fig. 2). At 32 weeks, diabetic *Mkk3*$^{+/+}$ *db/db* mice had increased kidney levels of phospho-p38, whereas the levels in diabetic *Mkk3*$^{-/-}$ *db/db* mice were not different from *db/+* controls (Fig. 3a,b). Similarly, the kidney levels of phospho-MKK3/6 were elevated in diabetic *Mkk3*$^{+/+}$ *db/db* mice at 32 weeks, whereas diabetic *Mkk3*$^{-/-}$ *db/db* mice showed a trend towards reduced levels of phospho-MKK3/6, which did not reach statistical significance (Fig. 3a,c). Diabetic *Mkk3*$^{+/+}$ *db/db* mice had a threefold increase in

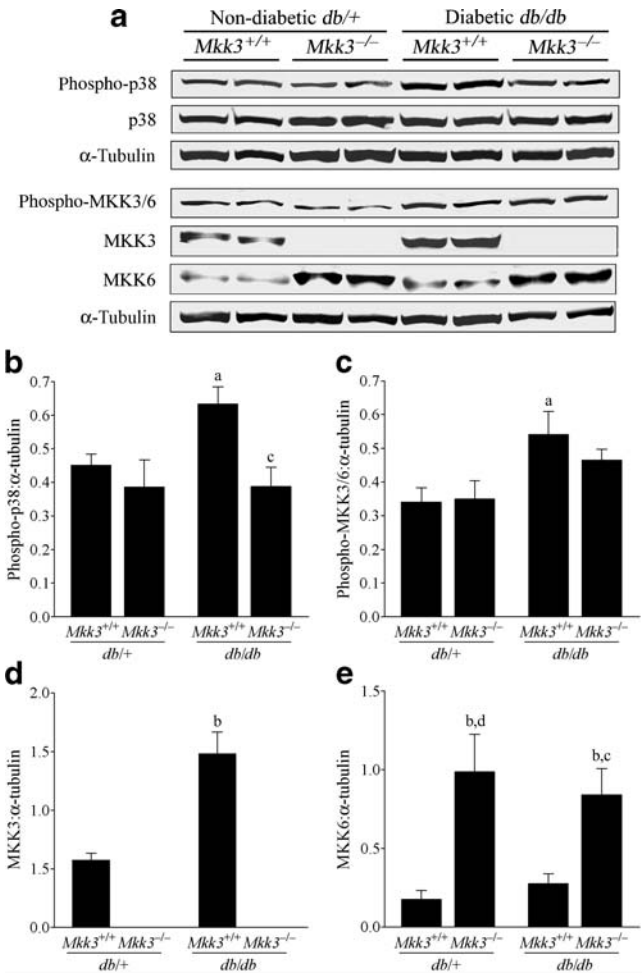

Fig. 3 Western blotting analysis of kidney p38 pathway activation. **a** Representative western blots showing protein bands of MKK3, MKK6 and p38, along with their associated phosphorylated protein bands. α-Tubulin was used as the loading control. **b** Quantification of phospho-p38 by densitometry showed a 35% reduction in kidney p38 phosphorylation in *Mkk3*$^{-/-}$ *db/db* compared with *Mkk3*$^{+/+}$ *db/db* mice. **c** Combined phospho-MKK3/6 protein increased in diabetes, but remained similar in both *Mkk3* genotypes of *db/db* mice, indicating high levels of MKK6 phosphorylation. **d** MKK3 protein bands were absent in *Mkk3*$^{-/-}$ mice, but MKK3 was significantly increased in *db/db* compared with *db/+* *Mkk3*$^{+/+}$ mice. **e** A compensatory increase in MKK6 was observed in *Mkk3*$^{-/-}$ mice, but diabetes as such was not associated with a significantly elevated MKK6 level. Data are means±SEM; $n=10$. Comparisons were made by one way ANOVA (**a–c**, **e**) and *t* test (**d**). [a]$p<0.05$, [b]$p<0.01$ vs *Mkk3*$^{+/+}$ *db/+* mice; [c]$p<0.05$, [d]$p<0.01$ vs *Mkk3*$^{+/+}$ *db/db* mice

kidney levels of MKK3 protein, but no change in MKK6 protein levels compared with *db/+* mice. Deficiency of *Mkk3* resulted in a compensatory increase in MKK6 protein levels in *db/+* and *db/db* mice compared with wild-type controls (Fig. 3d,e). This compensatory increase in kidney MKK6 protein levels did not increase kidney levels of phospho-p38 in the diabetic *Mkk3*$^{-/-}$ *db/db* mice.

Immunostaining of normal *db/+* mouse kidneys identified phospho-p38 in glomerular podocytes and collecting ducts (Fig. 4). In diabetic *Mkk3*$^{+/+}$ *db/db* mice, the number of phospho-p38-positive cells was significantly increased in the glomeruli, tubules and the interstitium compared with non-diabetic *db/+* controls (Fig. 4). The major sources of additional kidney phospho-p38 staining were dilated tubules, interstitial myofibroblasts and mesangial cells. At 32 weeks, diabetic *Mkk3*$^{-/-}$ *db/db* mice had 50% less phospho-p38-positive cells in glomeruli and tubules than diabetic *Mkk3*$^{+/+}$ *db/db* mice (Fig. 4), which is consistent with the western blot analysis of phospho-p38 in the total kidney.

Mkk3 deficiency reduces albuminuria and preserves renal function in db/db mice The urine albumin excretion of *db/+* mice remained stable at 5 mg/mmol creatinine between 8 and 32 weeks. In comparison, the urine albumin: creatinine ratio increased progressively in diabetic *Mkk3*$^{+/+}$ *db/db* mice and was 11-fold higher than in *db/+* counterparts at 32 weeks. This increase in the urine albumin:creatinine ratio was reduced by 70% in *Mkk3*$^{-/-}$ *db/db* mice at 32 weeks (Fig. 5a). Furthermore, at 32 weeks, a decline in creatinine clearance was seen in diabetic *Mkk3*$^{+/+}$ *db/db* mice compared with *db/+* mice; however, renal function was protected in the diabetic *Mkk3*$^{-/-}$ *db/db* mice (Fig. 5b).

Mkk3 deficiency reduces renal injury in diabetic db/db mice Wild-type *Mkk3*$^{+/+}$ *db/db* mice developed significant glomerular lesions at 32 weeks, which included glomerular hypertrophy, hypercellularity, increased mesangial matrix and collagen deposition. In comparison, *Mkk3*$^{-/-}$ *db/db* mice had similar glomerular hypertrophy and hypercellularity, but showed significant reductions in renal hypertrophy, glomerular matrix and collagen levels (Table 2). Immunostaining for WT1 demonstrated significant podocyte depletion in diabetic *Mkk3*$^{+/+}$ *db/db* mice compared with *db/+* mice, which was partially attenuated in diabetic *Mkk3*$^{-/-}$ *db/db* mice (Fig. 6). Podocyte numbers correlated inversely with the urine albumin: creatinine ratio associated with diabetes ($r=-0.65$, $p=0.0002$). Mesangial immunostaining of α-SMA, a marker of mesangial cell activation, was increased in *Mkk3*$^{+/+}$ *db/db* compared with *db/+* mice; however, this response was reduced in *Mkk3*$^{-/-}$ *db/db* mice (Fig. 6).

Significant tubulointerstitial lesions were also found in *Mkk3*$^{+/+}$ *db/db* mice at 32 weeks. These included tubular atrophy, tubular cell apoptosis, increased interstitial volume, accumulation of α-SMA-positive myofibroblasts and enhanced collagen deposition (Table 2, Fig. 7). Tubular cell proliferation, an index of the response to tubular damage, was also increased in these diabetic kidneys (Table 2). In

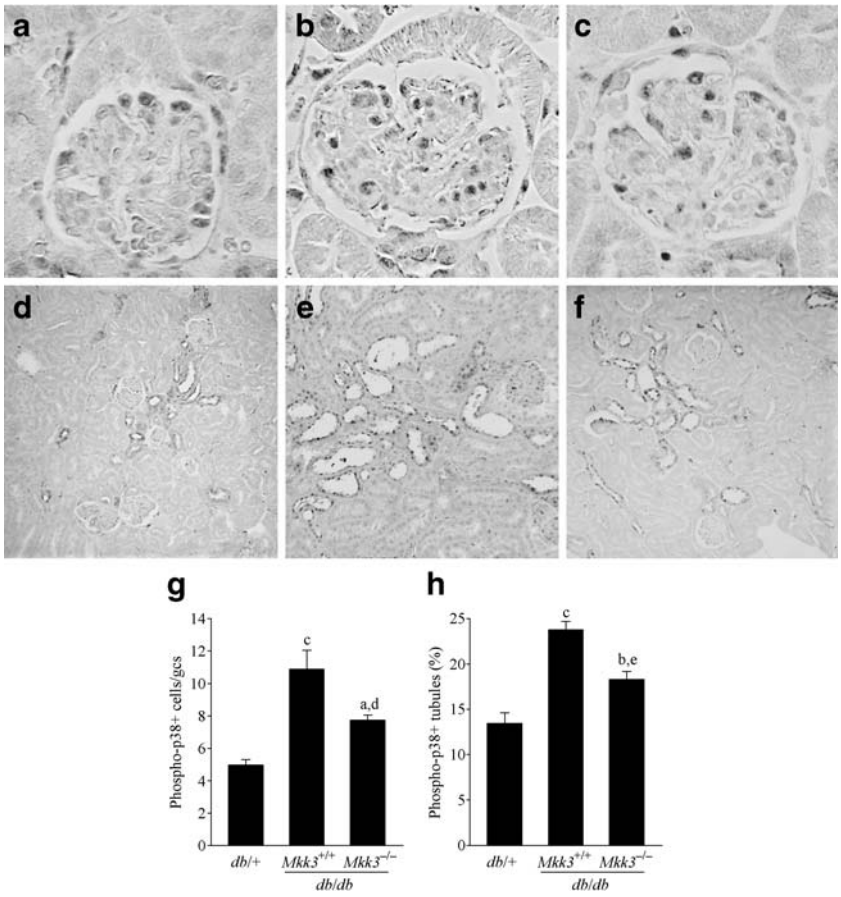

Fig. 4 Phospho-p38 immunohistochemistry. Immunostaining for phospho-p38 in the *db/+* kidney demonstrated normal phospho-p38 staining in the occasional podocyte and collecting ducts (**a**, **d**). In the *Mkk3*$^{+/+}$ *db/db* kidney, there was a twofold increase in glomerular and tubular staining for phospho-p38**,** particularly within the mesangium and dilated tubules (**b**, **e**, **g**, **h**). In the *Mkk3*$^{-/-}$ *db/db* kidney, the increased glomerular and tubular phospho-p38-positive cells were reduced by 50% (**c**, **f**, **g**, **h**). Magnification: **a–c** ×400; **d–f** ×160. Data are means±SEM; $n=10$. $^{a}p<0.05$, $^{b}p<0.01$, $^{c}p<0.001$ vs *db/+* mice; $^{d}p<0.05$, $^{e}p<0.01$ vs *Mkk3*$^{+/+}$ *db/db* mice

comparison, all measured markers of tubular injury and tubulointerstitial collagen deposition were significantly reduced in diabetic *Mkk3*$^{-/-}$ *db/db* mice (Table 2). There was also a trend towards reduced interstitial myofibroblast accumulation in *db/db* mice lacking *Mkk3*; however, this was not statistically significant.

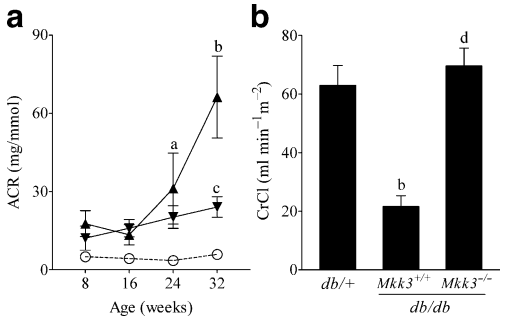

Fig. 5 Urinary albumin excretion and renal function. **a** Serial measurements of the albumin:creatinine ratio (ACR) from 8 to 32 weeks demonstrated a static ACR of around 5 mg/mmol in control *db/+* mice (circles). The ACR progressively increased in *Mkk3*$^{+/+}$ *db/db* mice (upright triangles) and was 11-fold greater than normal by 32 weeks. In contrast, the rise in ACR was significantly attenuated in *Mkk3*$^{-/-}$ *db/db* mice (inverted triangles). **b** Creatinine clearance (CrCl) was reduced in *Mkk3*$^{+/+}$ *db/db* mice compared with *db/+* mice, but this loss of renal function was abolished in *Mkk3*$^{-/-}$ *db/db* mice. Data are means±SEM; $n=10$. $^{a}p<0.05$, $^{b}p<0.001$ for *db/db* vs *db/+* mice; $^{c}p<0.05$, $^{d}p<0.001$ for *Mkk3*$^{-/-}$ *db/db* vs *Mkk3*$^{+/+}$ *db/db* mice

Gene transcript levels of proinflammatory and profibrotic molecules were also measured. *Ccl2* was examined because it is known to be increased in diabetic kidneys and promotes interstitial inflammation [35]. At 32 weeks, kidney *Ccl2* mRNA was increased more than threefold in diabetic *Mkk3*$^{+/+}$ *db/db* mice compared with *db/+* mice, but this upregulation of *Ccl2* was reduced by 50% in diabetic *Mkk3*$^{-/-}$ *db/db* mice (Fig. 8). The accumulation of interstitial CD68-positive macrophages, detected by immunostaining (Table 2), correlated with the increased level of kidney *Ccl2* mRNA in diabetic *Mkk3*$^{+/+}$ *db/db* mice and its reduction in diabetic *Mkk3*$^{-/-}$ *db/db* mice ($r=0.51$, $p=0.02$). In contrast, kidney mRNA levels of *Tgf-β1* and *Tnf-α* mRNA levels were increased three- to fourfold in diabetic *Mkk3*$^{+/+}$ *db/db* mice compared with *db/+* mice, but were not reduced in diabetic *Mkk3*$^{-/-}$ *db/db* mice (Fig. 8).

Discussion

This study has established a role for MKK3 and its effect on p38 MAPK signalling in the development of diabetic

Table 2 Renal pathology of selected diabetic *db/db* mice

Characteristic	Mouse genotype		
	db/+	*db/db*	
	Mkk3$^{+/+}$	*Mkk3*$^{+/+}$	*Mkk3*$^{-/-}$
Renal hypertrophy			
Kidney/body weight (%)	1.04±0.03	1.26±0.12	0.94±0.05[c]
Glomerular damage			
Volume ($\mu m^3 \times 10^4$)	18.1±0.7	36.3±3.8[a]	34.4±1.4[a]
Cellularity (cells/gcs)	34.5±1.0	48.7±2.3[a]	46.2±1.2[a]
Matrix fraction (% area)	20.3±1.0	29.8±2.6[b]	27.0±3.2[b,c]
Collagen (% area)	17.7±1.0	25.9±0.8[b]	21.1±0.6[a,e]
Proliferation (cells/gcs)	0.32±0.05	0.95±0.21[a]	0.49±0.14
Macrophages (cells/gcs)	1.1±0.4	5.3±0.9[a]	4.4±0.9
Tubular damage			
Atrophy (% tubules)	0.33±0.04	4.93±0.63[b]	2.23±0.29[a,e]
Apoptosis (cells/mm^2)	0.25±0.03	0.46±0.07[a]	0.27±0.03[c]
Proliferation (cells/mm^2)	15.2±1.5	25.0±4.4[a]	9.2±2.6[d]
Interstitial damage			
α-SMA (% area)	0.77±0.13	3.71±0.75[a]	2.07±0.58
Collagen (% area)	2.86±0.24	4.51±0.35[b]	3.24±0.40[c]
Interstitial volume (% points)	3.37±0.21	6.70±0.44[b]	5.94±0.50[b]
Proliferation (cells/mm^2)	12.4±1.2	19.1±4.1	13.0±3.5
Macrophages (cells/mm^2)	72±7	143±10[b]	111±8[c]

Data are mean±SEM, $n=10$
[a] $p<0.05$, [b] $p<0.001$ vs control *db/+* mice
[c] $p<0.05$, [d] $p<0.01$, [e] $p<0.001$ vs *Mkk3*$^{+/+}$ *db/db* mice

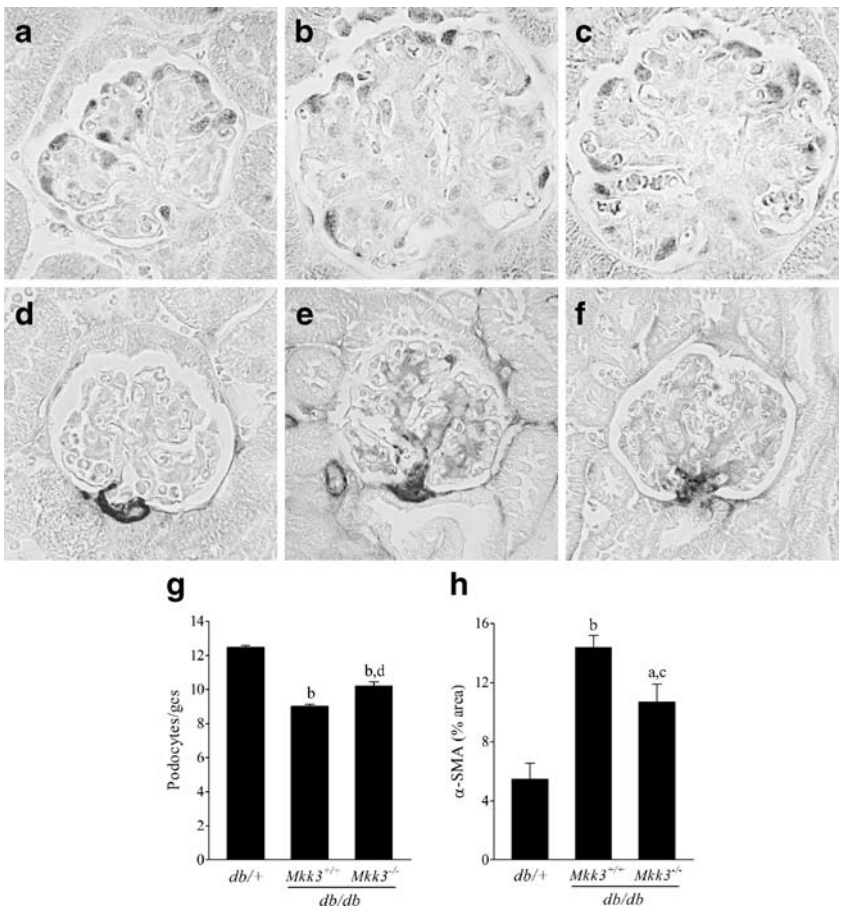

Fig. 6 Effect of *Mkk3* deficiency on podocyte depletion and mesangial cell activation. WT1 immunostaining for podocytes in control *db/+* (**a**), *Mkk3*$^{+/+}$ *db/db* (**b**) and *Mkk3*$^{-/-}$ *db/db* mice (**c**) demonstrated a marked reduction in podocyte numbers in *Mkk3*$^{+/+}$ diabetic mice, which was better preserved in *Mkk3*$^{-/-}$ diabetic mice (**g**). Immunostaining for α-SMA as a marker of mesangial cell activation in *db/+* mice (**d**), *Mkk3*$^{+/+}$ *db/db* mice (**e**) and *Mkk3*$^{-/-}$ *db/db* mice (**f**) demonstrated a small amount of age-related α-SMA in *db/+* mice, which was dramatically increased in *Mkk3*$^{+/+}$ *db/db* mice and attenuated in *Mkk3*$^{-/-}$ *db/db* mice. Magnification: **a–c** ×1,000; **d–f** ×400. Data are means±SEM; $n=10$. [a] $p<0.01$, [b] $p<0.001$ vs *db/+* mice; [c] $p<0.05$, [d] $p<0.001$ vs *Mkk3*$^{+/+}$ *db/db* mice

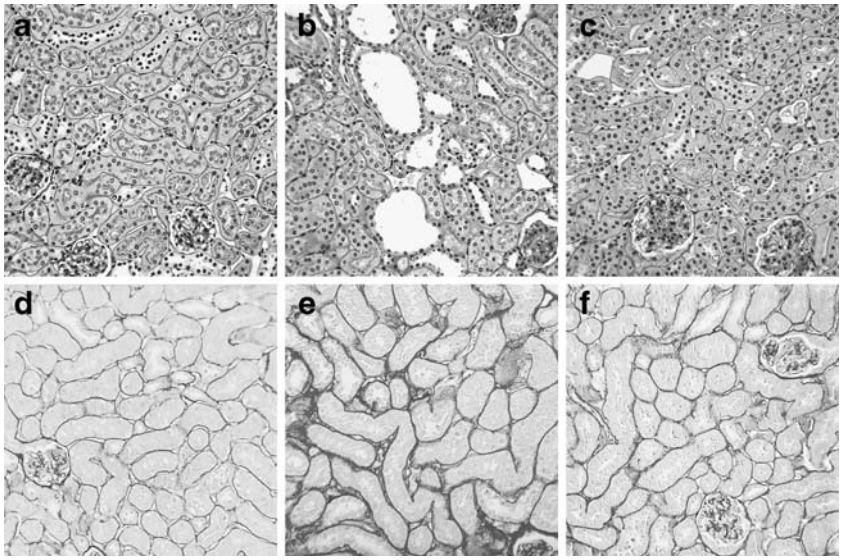

Fig. 7 Tubulo-interstitial injury is reduced by *Mkk3* deficiency. Periodic acid–Schiff's reagent sections of *db/+* (**a**), *Mkk3*$^{+/+}$ *db/db* (**b**) and *Mkk3*$^{-/-}$ *db/db* (**c**) mice demonstrated that tubular atrophy was greatly increased in diabetes, but significantly improved in *Mkk3*$^{-/-}$ *db/db* mice. Sirius Red staining of collagen in *db/+* (**d**), *Mkk3*$^{+/+}$ *db/db* (**e**) and *Mkk3*$^{-/-}$ *db/db* mice (**f**) demonstrated that diabetic mice developed significant thickening of the tubular basement membrane and increased interstitial collagen, but both of these were reduced in *Mkk3*$^{-/-}$ *db/db* mice. Magnification: ×250

nephropathy in *db/db* mice. Although *Mkk3* deficiency did not alter the incidence or progression of obesity and type 2 diabetes, it did significantly reduce diabetic renal injury and prevented a loss of renal function in our model, indicating that MKK3–p38 signalling is important to the pathology of diabetic nephropathy.

Previous studies had led us to anticipate that *Mkk3* deficiency would modify the major metabolic events leading to type 2 diabetes. In vitro experiments have shown that p38 activation reduces expression of the glucose transporter GLUT4 [7, 36] and suppresses adipogenesis by inhibiting *Ppar-γ* (also known as *Pparg*) and *c/ebp-β* (also known as *Cebpb*) transcriptional activities [37], suggesting that a deficiency of MKK3–p38 signalling might promote insulin-stimulated glucose uptake and adipose expansion. However, our study showed that *Mkk3* deficiency did not affect body weight, insulin and glucose tolerance, plasma insulin or epididymal fat accumulation. There was a small difference in liver size, which may be related to reduced hepatic lipogenesis [38], but serum NEFA were unaffected and no observable effect on hyperglycaemia was seen, as demonstrated by the equivalent incidence of type 2 diabetes and similar fasting blood glucose and glycated haemoglobin values in both genotypes. Thus, our findings prove that MKK3–p38 signalling is not by itself critical to the development of obesity or type 2 diabetes and that compensatory mechanisms may exist to overcome any decline in p38 activity in *Mkk3*$^{-/-}$ tissues regulating obesity and hyperglycaemia.

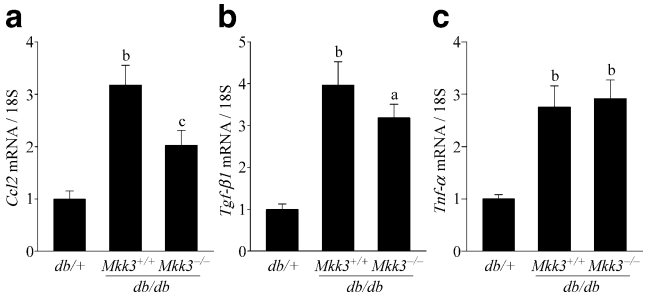

Fig. 8 *Mkk3* deficiency attenuates kidney expression of *Ccl2* but not *Tgf-β1* or *Tnf-α*. Assessment of kidney expression of *Ccl2* by quantitative RT-PCR (**a**) demonstrated a threefold increase in *Ccl2* mRNA in *Mkk3*$^{+/+}$ *db/db* compared with control *db/+* mice, which was reduced by 50% in *Mkk3*$^{-/-}$ *db/db* mice. Kidney expression of *Tgf-β1* (**b**) and *Tnf-α* mRNA (**c**) was increased four- and threefold, respectively, in *db/db* mice, compared with control *db/+* mice, and was not significantly affected by *Mkk3* deficiency. Data are means± SEM; $n=10$. $^{a}p<0.05$, $^{b}p<0.01$ vs *db/+* mice; $^{c}p<0.05$ vs *Mkk3*$^{+/+}$ *db/db* mice

Our examination of *Mkk3*$^{+/+}$ *db/db* mice established that kidney MKK3 levels are increased in type 2 diabetes in association with elevated p38 MAPK signalling. *Mkk3* deficiency prevented this increase in kidney p38 MAPK signalling despite a compensatory increase in MKK6. This phenomenon has also been observed in *Mkk3*$^{-/-}$ kidneys with obstructive uropathy [39] and is consistent with an in vitro study showing that inhibition of p38α stimulates MKK6 production [40].

Histopathology analysis demonstrated that MKK3–p38 signalling contributes to early glomerular injury in diabetic *db/db* kidneys. Podocyte depletion is a characteristic feature of diabetic nephropathy, both in experimental models [16] and in human type 2 diabetes [41–43], and is associated with the development of albuminuria. In this study, we saw preservation of podocyte numbers in the diabetic kidneys of *Mkk3*$^{-/-}$ compared with *Mkk3*$^{+/+}$ *db/db* mice, a finding which correlated with protection from albuminuria. This finding supports in vitro observations that activation of p38 by AGE and oxidative stress triggers podocyte apoptosis [16, 21, 28]. However, significant protection from podocyte apoptosis was not observed in our model because podocyte

apoptosis is an early response to hyperglycaemia [16] and our *db/db* mice were examined after 20 weeks of hyperglycaemia. Deficiency of *Mkk3* also reduced glomerular levels of α-SMA and collagen in diabetic *db/db* kidneys, which is consistent with in vitro observations showing that TGF-β1-induced collagen production by murine mesangial cells is dependent on MKK3–p38 signalling [30]. This finding is clinically relevant, since mesangial cell production of α-SMA correlates with glomerulosclerosis in human type 2 diabetes [44].

In diabetic *Mkk3*$^{-/-}$ *db/db* mice, protection against tubulointerstitial damage also coincided with a reduction in albuminuria. Elements of the diabetic milieu (hyperglycaemia and AGE) as well as albuminuria are capable of causing tubular injury, which may occur via the activation of p38 signalling. However, here we were unable to distinguish whether one or both of these mechanisms were affected by a deficiency of *Mkk3* in our model.

Increased levels of the *Ccl2* gene and its protein MCP-1 are consistently found in diabetic kidneys and are required for the progression of renal inflammation and injury [35, 45]. In this study, *Mkk3*$^{-/-}$ *db/db* mice had reduced kidney expression of *Ccl2* mRNA, which correlated with a similar reduction in interstitial macrophages, suggesting that the inflammatory process had been suppressed. In addition, reduced *Ccl2* expression may also directly impact on glomerulosclerosis since MCP-1 induces fibronectin production in human mesangial cells, which are known to possess the MCP-1 receptor, and *Ccl2* deficiency results in reduced glomerular fibronectin deposition in diabetic kidneys [46]. This potential mechanism is supported by our finding that diabetic *Mkk3*$^{-/-}$ kidneys are partially protected from glomerular fibrosis, as well as by a recent study showing that suppression of p38 activity reduces fibronectin production in diabetic glomeruli [47]. Therefore, this study has identified that MKK3–p38 signalling is a factor promoting MCP-1-mediated injury in diabetic kidneys, which is consistent with other models of kidney disease showing that inhibition of p38 signalling suppresses abnormal renal MCP-1 production [13].

In diabetic *db/db* kidneys, *Mkk3* deficiency did not reduce mRNA expression of *Tgf-β1* and *Tnf-α*, suggesting that p38 signalling is either not necessary or that the compensatory increase in MKK6–p38 signalling is sufficient to promote renal production of these cytokines. Evidence for this comes from in vitro studies. Although p38 inhibitors can inhibit IL-1 and TNF-α production by macrophages [48], production of IL-1, IL-6 and TNF-α is not affected in *Mkk3*$^{-/-}$ macrophages stimulated with lipopolysaccharide [49]. Thus, the dependence of renal cytokine production on MKK3–p38 signalling may vary according to the stimulus, cell type and the level of p38 activation required. One noteworthy finding in this study is that *Mkk3* deficiency reduced renal fibrosis in diabetic *db/db* mice without lowering kidney expression of *Tgf-β1* mRNA. Blockade of p38α has also been reported to reduce acute renal fibrosis without affecting *Tgf-β1* mRNA or protein in a rat model of unilateral ureteric obstruction [50]. These findings together suggest that MKK3–p38 signalling plays a role in the development of renal fibrosis by acting downstream of TGF-β1.

In conclusion, MKK3–p38 signalling is not required for the development of obesity or type 2 diabetes, but does play a significant role in the progression of diabetic nephropathy in *db/db* mice.

Acknowledgements We thank N. Gibson, Y. Han, P. Frost and E. Grixti for their technical assistance. This study was funded by the National Health and Medical Research Council of Australia and Kidney Health Australia.

Duality of interest The authors declare that there is no duality of interest associated with this manuscript.

References

1. Sheetz MJ, King GL (2002) Molecular understanding of hyperglycemia's adverse effects for diabetic complications. Jama 288:2579–2588
2. Zarubin T, Han J (2005) Activation and signaling of the p38 MAP kinase pathway. Cell Res 15:11–18
3. Cuenda A, Rousseau S (2007) p38 MAP-kinases pathway regulation, function and role in human diseases. Biochim Biophys Acta 1773:1358–1375
4. Furtado LM, Somwar R, Sweeney G, Niu W, Klip A (2002) Activation of the glucose transporter GLUT4 by insulin. Biochem Cell Biol = Biochimie et Biologie Cellulaire 80:569–578
5. Adhikary L, Chow F, Nikolic-Paterson DJ et al (2004) Abnormal p38 mitogen-activated protein kinase signalling in human and experimental diabetic nephropathy. Diabetologia 47:1210–1222
6. Koistinen HA, Chibalin AV, Zierath JR (2003) Aberrant p38 mitogen-activated protein kinase signalling in skeletal muscle from Type 2 diabetic patients. Diabetologia 46:1324–1328
7. Carlson CJ, Koterski S, Sciotti RJ, Poccard GB, Rondinone CM (2003) Enhanced basal activation of mitogen-activated protein kinases in adipocytes from type 2 diabetes: potential role of p38 in the downregulation of GLUT4 expression. Diabetes 52:634–641
8. Westermann D, Rutschow S, Van Linthout S et al (2006) Inhibition of p38 mitogen-activated protein kinase attenuates left ventricular dysfunction by mediating pro-inflammatory cardiac cytokine levels in a mouse model of diabetes mellitus. Diabetologia 49:2507–2513
9. Ando H, Kurita S, Takamura T (2004) The specific p38 mitogen-activated protein kinase pathway inhibitor FR167653 keeps insulitis benign in nonobese diabetic mice. Life Sci 74:1817–1827
10. Aouadi M, Jager J, Laurent K et al (2007) p38MAP kinase activity is required for human primary adipocyte differentiation. FEBS lett 581:5591–5596

11. Carlson CJ, Rondinone CM (2005) Pharmacological inhibition of p38 MAP kinase results in improved glucose uptake in insulin-resistant 3T3-L1 adipocytes. Metabolism 54:895–901
12. Sakai N, Wada T, Furuichi K et al (2005) Involvement of extracellular signal-regulated kinase and p38 in human diabetic nephropathy. Am J Kidney Dis 45:54–65
13. Sheryanna A, Bhangal G, McDaid J et al (2007) Inhibition of p38 mitogen-activated protein kinase is effective in the treatment of experimental crescentic glomerulonephritis and suppresses monocyte chemoattractant protein-1 but not IL-1beta or IL-6. J Am Soc Nephrol 18:1167–1179
14. Stambe C, Atkins RC, Tesch GH et al (2003) Blockade of p38alpha MAPK ameliorates acute inflammatory renal injury in rat anti-GBM glomerulonephritis. J Am Soc Nephrol 14:338–351
15. Wilmer WA, Dixon CL, Hebert C (2001) Chronic exposure of human mesangial cells to high glucose environments activates the p38 MAPK pathway. Kidney Int 60:858–871
16. Susztak K, Raff AC, Schiffer M, Bottinger EP (2006) Glucose-induced reactive oxygen species cause apoptosis of podocytes and podocyte depletion at the onset of diabetic nephropathy. Diabetes 55:225–233
17. Zhang SL, Tang SS, Chen X, Filep JG, Ingelfinger JR, Chan JS (2000) High levels of glucose stimulate angiotensinogen gene expression via the P38 mitogen-activated protein kinase pathway in rat kidney proximal tubular cells. Endocrinology 141:4637–4646
18. Daoud S, Schinzel R, Neumann A et al (2001) Advanced glycation endproducts: activators of cardiac remodeling in primary fibroblasts from adult rat hearts. Mol Med 7:543–551
19. Liu BF, Miyata S, Hirota Y et al (2003) Methylglyoxal induces apoptosis through activation of p38 mitogen-activated protein kinase in rat mesangial cells. Kidney Int 63:947–957
20. Kang YS, Park YG, Kim BK et al (2006) Angiotensin II stimulates the synthesis of vascular endothelial growth factor through the p38 mitogen activated protein kinase pathway in cultured mouse podocytes. J Mol Endocrinol 36:377–388
21. Chuang PY, Yu Q, Fang W, Uribarri J, He JC (2007) Advanced glycation endproducts induce podocyte apoptosis by activation of the FOXO4 transcription factor. Kidney Int 72:965–976
22. Porras A, Zuluaga S, Black E et al (2004) P38 alpha mitogen-activated protein kinase sensitizes cells to apoptosis induced by different stimuli. Mol Biol Cell 15:922–933
23. Takaishi H, Taniguchi T, Takahashi A, Ishikawa Y, Yokoyama M (2003) High glucose accelerates MCP-1 production via p38 MAPK in vascular endothelial cells. Biochem Biophys Res Commun 305:122–128
24. Suzuki H, Uchida K, Nitta K, Nihei H (2004) Role of mitogen-activated protein kinase in the regulation of transforming growth factor-beta-induced fibronectin accumulation in cultured renal interstitial fibroblasts. Clin Exp Neurol 8:188–195
25. Chin BY, Mohsenin A, Li SX, Choi AM, Choi ME (2001) Stimulation of pro-alpha(1)(I) collagen by TGF-beta(1) in mesangial cells: role of the p38 MAPK pathway. Am J Physiol Renal Physiol 280:F495–F504
26. Fujita H, Omori S, Ishikura K, Hida M, Awazu M (2004) ERK and p38 mediate high-glucose-induced hypertrophy and TGF-beta expression in renal tubular cells. Am J Physiol Renal Physiol 286: F120–F126
27. Wu DT, Bitzer M, Ju W, Mundel P, Bottinger EP (2005) TGF-beta concentration specifies differential signaling profiles of growth arrest/differentiation and apoptosis in podocytes. J Am Soc Nephrol 16:3211–3221
28. Schiffer M, Bitzer M, Roberts IS et al (2001) Apoptosis in podocytes induced by TGF-beta and Smad7. J Clin Invest 108:807–816
29. Zhuang S, Yan Y, Han J, Schnellmann RG (2005) p38 kinase-mediated transactivation of the epidermal growth factor receptor is required for dedifferentiation of renal epithelial cells after oxidant injury. J Biol Chem 280:21036–21042
30. Wang L, Ma R, Flavell RA, Choi ME (2002) Requirement of mitogen-activated protein kinase kinase 3 (MKK3) for activation of p38alpha and p38delta MAPK isoforms by TGF-beta 1 in murine mesangial cells. J Biol Chem 277:47257–47262
31. Wang L, Kwak JH, Kim SI, He Y, Choi ME (2004) Transforming growth factor-beta1 stimulates vascular endothelial growth factor 164 via mitogen-activated protein kinase kinase 3-p38alpha and p38delta mitogen-activated protein kinase-dependent pathway in murine mesangial cells. J Biol Chem 279:33213–33219
32. Inoue T, Boyle DL, Corr M et al (2006) Mitogen-activated protein kinase kinase 3 is a pivotal pathway regulating p38 activation in inflammatory arthritis. Proc Natl Acad Sci U S A 103:5484–5489
33. Fukuda K, Tesch GH, Yap FY et al (2008) MKK3 signalling plays an essential role in leukocyte-mediated pancreatic injury in the multiple low-dose streptozotocin model. Lab Invest 88:398–407
34. Wysk M, Yang DD, Lu HT, Flavell RA, Davis RJ (1999) Requirement of mitogen-activated protein kinase kinase 3 (MKK3) for tumor necrosis factor-induced cytokine expression. Proc Natl Acad Sci U S A 96:3763–3768
35. Chow FY, Nikolic-Paterson DJ, Ma FY, Ozols E, Rollins BJ, Tesch GH (2007) Monocyte chemoattractant protein-1-induced tissue inflammation is critical for the development of renal injury but not type 2 diabetes in obese db/db mice. Diabetologia 50:471–480
36. Fujishiro M, Gotoh Y, Katagiri H et al (2001) MKK6/3 and p38 MAPK pathway activation is not necessary for insulin-induced glucose uptake but regulates glucose transporter expression. J Biol Chem 276:19800–19806
37. Aouadi M, Laurent K, Prot M, Le Marchand-Brustel Y, Binetruy B, Bost F (2006) Inhibition of p38MAPK increases adipogenesis from embryonic to adult stages. Diabetes 55:281–289
38. Xiong Y, Collins QF, An J et al (2007) p38 mitogen-activated protein kinase plays an inhibitory role in hepatic lipogenesis. J Biol Chem 282:4975–4982
39. Ma FY, Tesch GH, Flavell RA, Davis RJ, Nikolic-Paterson DJ (2007) MKK3-p38 signaling promotes apoptosis and the early inflammatory response in the obstructed mouse kidney. Am J Physiol Renal Physiol 293:F1556–F1563
40. Ambrosino C, Mace G, Galban S et al (2003) Negative feedback regulation of MKK6 mRNA stability by p38alpha mitogen-activated protein kinase. Mol Cell Biol 23:370–381
41. Dalla Vestra M, Masiero A, Roiter AM, Saller A, Crepaldi G, Fioretto P (2003) Is podocyte injury relevant in diabetic nephropathy? Studies in patients with type 2 diabetes. Diabetes 52:1031–1035
42. Pagtalunan ME, Miller PL, Jumping-Eagle S et al (1997) Podocyte loss and progressive glomerular injury in type II diabetes. J Clin Invest 99:342–348
43. Verzola D, Gandolfo MT, Ferrario F et al (2007) Apoptosis in the kidneys of patients with type II diabetic nephropathy. Kidney Int 72:1262–1272
44. Yonemoto S, Machiguchi T, Nomura K, Minakata T, Nanno M, Yoshida H (2006) Correlations of tissue macrophages and cytoskeletal protein expression with renal fibrosis in patients with diabetes mellitus. Clin Exp Neurol 10:186–192
45. Tesch GH (2008) MCP-1/CCL2: a new diagnostic marker and therapeutic target for progressive renal injury in diabetic nephropathy. Am J Physiol Renal Physiol 294:F607–F701
46. Giunti S, Tesch GH, Pinach S et al (2008) Monocyte chemoattractant protein-1 has prosclerotic effects both in a mouse model of experimental diabetes and in vitro in human mesangial cells. Diabetologia 51:198–207

47. Jung DS, Li JJ, Kwak SJ et al (2008) FR167653 inhibits fibronectin expression and apoptosis in diabetic glomeruli and in high-glucose-stimulated mesangial cells. Am J Physiol Renal Physiol 295:F595–F604
48. Lee JC, Laydon JT, McDonnell PC et al (1994) A protein kinase involved in the regulation of inflammatory cytokine biosynthesis. Nature 372:739–746
49. Lu HT, Yang DD, Wysk M et al (1999) Defective IL-12 production in mitogen-activated protein (MAP) kinase kinase 3 (Mkk3)-deficient mice. EMBO J 18:1845–1857
50. Stambe C, Atkins RC, Tesch GH, Masaki T, Schreiner GF, Nikolic-Paterson DJ (2004) The role of p38alpha mitogen-activated protein kinase activation in renal fibrosis. J Am Soc Nephrol 15:370–379